Effects of exciton–acoustic-phonon scattering on optical line shapes and exciton dephasing in semiconductors and semiconductor quantum wells

S. Rudin
U.S. Army Research Laboratory, Adelphi, Maryland 20783

T. L. Reinecke
Naval Research Laboratory, Washington, D.C. 20375
(Received 5 December 2001; published 16 August 2002)

The interaction of excitons with acoustic phonons in direct band-gap semiconductors gives the dominant contribution to the temperature-dependent part of the exciton homogeneous linewidths and to dephasing rates at lower temperatures, e.g., below 150 K in bulk GaAs. Experimental results have shown that this contribution increases substantially in going from GaAs quantum wells to bulk GaAs. A perturbation treatment of acoustic phonon scattering in a simple band exciton model—i.e., neglecting valence-band coupling and anisotropy of exciton dispersion—agrees with experimental results in narrow quantum wells. On the other hand, it fails by an order of magnitude for bulk GaAs and by a large factor for other materials. Here we give a thorough theoretical discussion of this problem. The exciton linewidth is calculated to lowest order in the exciton–acoustic-phonon coupling including valence-band interactions and anisotropic exciton dispersion. The effects of multiple scatterings of phonons in higher orders of the exciton-phonon interactions are calculated and previous work on these effects are discussed. The effects of impurity motion from acoustic phonons on the exciton linewidths are evaluated. We conclude that the temperature-dependent exciton linewidth is given reasonably well by the lowest-order phonon scatterings provided that the full anisotropic exciton dispersion is included. Higher-order phonon scatterings give a small contribution to the linewidth and can affect the line shape. These results agree well with available experimental results for the low-temperature exciton linewidths in bulk GaAs and ZnSe and in quantum wells from these materials.

DOI: 10.1103/PhysRevB.66.085314 PACS number(s): 78.20.−e, 78.67.De, 71.35.Cc

I. INTRODUCTION

The interaction of excitons with acoustic phonons in direct band-gap semiconductors gives the dominant contribution to the temperature-dependent part of the exciton homogeneous linewidths and dephasing rates at lower temperature, e.g., below 150 K in bulk GaAs.[1,2] There has been much interest in the effects of confinement on exciton broadening and dephasing.[1,3,4,5] Some understanding of confinement effects on the exciton-phonon interaction can be obtained by comparing exciton linewidths in quantum wells to the corresponding bulk values. In relatively narrow wells—say, narrower than 100 Å—the splitting of the valence band into heavy- and light-hole bands at the Γ point is sufficiently large to justify an evaluation of the exciton-phonon matrix elements in a simple band model—i.e., neglecting light–heavy-hole coupling. If carrier tunneling into the barriers is taken into account, this model gives exciton–acoustic-phonon scattering rates that are in overall agreement with experimentally deduced rates.[3–6] In bulk materials, on the other hand, the simple band model for a ''heavy-hole exciton'' [7] gives exciton–acoustic-phonon scattering rates that are an order of magnitude smaller than the values deduced from the experimentally measured linewidths.[8] A satisfactory quantitative theory for the exciton–acoustic-phonon scattering in bulk materials is required for an understanding of confinement effects on exciton linewidths, exciton dephasing and dissipation effects in optical quasimodes in semiconductor microcavities,[9] and exciton-polariton photoluminescence in bulk microcavities.[10]

Several possibilities have been suggested to address this discrepancy between experiment and theory for the bulk linewidth, including higher-order phonon scattering within an effective elastic approximation for the phonon scattering,[7] polariton effects on exciton dispersion,[8] contributions from the shear components of the deformation potential interaction,[3] and the effects of self-consistency in the broadening of the final states.[3] In this work we address this in detail theoretically. We develop fully the linewidth to lowest order in the exciton-phonon scattering including valence-band coupling and the resulting nonparabolic exciton dispersion. We give the effects of multiple-phonon scattering in higher orders of the exciton-phonon interaction and discuss the region of validity of the approach given in Ref. 7. We also consider the effects of self-enegy corrections arising from impurity motion due to phonons.

First, consider exciton phonon scattering to lowest order. The exciton–acoustic-phonon scattering rates in direct band-gap bulk semiconductors with cubic structure are evaluated to lowest order, taking the degeneracy of the valence band at the zone center and the anisotropy of the exciton dispersion into account. Theoretical models for excitons in which band degeneracy is taken into account will be referred to as ''complex band models.'' Both deformation potential (DP) and piezoelectric (PE) interactions with acoustic phonons are included. The resulting scattering rate gives the acoustic phonon contribution to the exciton dephasing rate and also determines the homogeneous linewidth of the absorption evaluated to the lowest order in the interaction strength—i.e., the Fermi golden rule (FGR) in the time-dependent perturba-

tion theory[11] with a thermal average over the phonon distribution taken. Here we define the linewidth as the half-width at half-maximum (HWHM) of the absorption. The use of the FGR is equivalent to the one-phonon process approximation in the evaluation of the exciton self-energy,[12] resulting in an approximately linear temperature dependence of the scattering rate, except at very low temperature. The matrix elements for DP and PE interactions are out of phase—i.e., one is real and the other is imaginary[13]—and they do not interfere to the lowest order. Therefore the corresponding linewidth to this order is the sum of the two contributions,

$$\Gamma = \Gamma(0) + \Gamma^{\mathrm{DP}} + \Gamma^{\mathrm{PE}} = \Gamma(0) + d_{\mathrm{ac}} T, \tag{1}$$

where $\Gamma(0)$ denotes the temperature-independent part and may arise from impurity scattering in the bulk case.

For detailed evaluations we consider two materials, GaAs and ZnSe. In both cases, the heavy-exciton dispersion is strongly anisotropic in reciprocal space.[14] The exciton radius in GaAs is about 3.3 times larger than in ZnSe. It turns out that the size of the exciton in a complex band material (i.e., including coupling in the valence band and thus anisotropy in the exciton dispersion) is an important factor in determining the relative contribution of DP and PE interactions to the scattering rates. In addition, the piezoelectric tensor components for ZnSe are much smaller than those for GaAs. In the simple band model of the ''heavy-hole exciton,'' using an effective-mass approximation near the zone center, the center-of-mass (COM) motion and the relative motion of the conduction-band electron with mass m_c and the valence-band hole with mass m_v can be separated exactly by a COM transformation. The exciton then has a mass $M = m_c + m_v$, a reduced mass $\mu = m_c m_v/(m_c + m_v)$, a total momentum $\hbar K$, and an effective Bohr radius $a_0 = 4\pi\bar{\varepsilon}\hbar^2/\mu e^2$, where e is electron charge, $1.602\,19 \times 10^{-19}$ C. The permittivity of the semiconductor $\bar{\varepsilon} = \varepsilon\varepsilon_f$, with ε_f being the permittivity in free space, 8.854×10^{-12} F/m, and ε is the static dielectric constant. The deformation potential for the conduction band is a scalar D_c and the deformation potential tensor for the valence band is replaced by an effective scalar D_v. For the ground-state exciton with initial momentum $\hbar K_{\mathrm{in}} \approx 0$, the final momentum $\hbar K$, as determined by the energy conservation in one-phonon absorption, is given by $K = 2Mv_{\mathrm{LA}}/\hbar$, where v_{LA} is the speed of sound for the longitudinal phonons. The resulting linewidths in the FGR simple band approximation are easily obtained,[8] and the DP and PE terms in Eq. (1) are given by

$$\Gamma_0^{\mathrm{DP}}/k_B T = \frac{M^2}{\pi v_{\mathrm{LA}} \hbar^3 \rho} \times \left[\frac{D_c}{(1 + a_0^2 \alpha_{0h}^2 K^2/4)^2} - \frac{D_v}{(1 + a_0^2 \alpha_{0e}^2 K^2/4)^2} \right]^2, \tag{2}$$

$$\Gamma_0^{\mathrm{PE}}/k_B T = \frac{e_{14}^2 e^2}{70\pi\bar{\varepsilon}^2 \rho \hbar} \left(\frac{3}{v_{\mathrm{LA}}^3} + \frac{4}{v_{\mathrm{TA}}^3} \right) \times \left[\frac{1}{(1 + a_0^2 \alpha_{0h}^2 K^2/4)^2} - \frac{1}{(1 + a_0^2 \alpha_{oe}^2 K^2/4)^2} \right]^2, \tag{3}$$

where the parameters of the COM transformation α_{0e} and α_{0h} in the simple band model are given by $\alpha_{0e} = m_c/M$, $\alpha_{0h} = m_v/M$, e_{14} is a component of the piezoelectric tensor, ρ is the material density, and v_{TA} is the speed of sound for the transverse phonons. SI units are used here.

In a simple valence-band model $a_0 K$ is small, and the exciton form factors, the expressions in the square brackets in Eqs. (2) and (3), can be replaced by $(D_c\text{-}D_v)$ for DP and 0 for PE. Therefore, the contribution of the piezoelectric scattering is negligible in a simple band model. On the other hand, in a complex band model the corresponding factors are given by more complicated expressions that take the anisotropy of the exciton dispersion into account. If one defines an effective anisotropic exciton mass $M(\hat{\mathbf{K}})$, its values for some directions will be significantly larger than M defined in a simple band model.[14,15] The values of K in some directions will not be small, and the electron and hole contributions in Γ^{PE} do not necessary cancel, unless the effective exciton radius is small.

In Sec. II we formulate the exciton linewidth problem by considering exciton states involved in the evaluation of the exciton-phonon interaction matrix elements based on a Kohn-Luttinger Hamiltonian for the valence band. There and in Appendix A we redefine the problem in terms of exciton states and also discuss a choice of the electron-hole coordinate transformation convenient for the exciton-phonon scattering problem. The exciton-phonon matrix elements are evaluated in Sec. III and used for the evaluation of the optical linewidth in the FGR approximation. The effects of multiple-phonon scatterings and the resulting absorption line shapes are evaluated in Sec. IV and Appendix B. We find that these combined multiphonon terms have only a small effect on the linewidth and that the temperature dependence of the calculated linewidth agrees well with the available experimental results. On the other hand, we find that the multiphonon terms have a noticeable effect on the line shape at higher temperatures. The effects of exciton-impurity scattering and possible impurity effects on exciton-phonon scattering are also considered there and in Appendix C. The exciton-phonon scattering in GaAs and ZnSe quantum wells is considered in Sec. V. A short version of the present work dealing with the FGR calculation has been given earlier.[16] The present paper gives fuller details of these calculations for the FGR and also discusses the multiphonon and impurity effects.

II. EXCITONS IN DIRECT BAND-GAP BULK SEMICONDUCTORS WITH DEGENERATE VALENCE BANDS

We obtain an effective-mass exciton Hamiltonian in a cubic semiconductor[15,17,18] using a simple isotropic conduction band, the Kohn-Luttinger Hamiltonian[19] for the valence band, and a statically screened electron-hole Coulomb interaction:

$$H_{e\text{-}h} = \frac{p_e^2}{2m_c} - \frac{e^2}{4\pi\varepsilon\varepsilon_f |\mathbf{r}_e - \mathbf{r}_h|} - H_v, \tag{4}$$

TABLE I. Values of the band parameters (Ref. 43) used in the calculation and the effective ground-state exciton radius calculated in the spherical model.

	m_c/m_0	γ_1	γ_2	γ_3	$a_{\rm exc}$ (Å)
GaAs	0.067	6.85	2.10	2.90	134.9
ZnSe	0.16	4.30	1.14	1.84	44.4

[a]Reference 43.

$$-H_v=\frac{p_h^2}{2m_0}\left(\gamma_1+\frac{5}{2}\gamma_2\right)-\frac{\gamma_2}{m_0}(p_{hx}^2J_x^2+p_{hy}^2J_y^2+p_{hz}^2J_z^2)$$
$$-\frac{2\gamma_3}{m_0}(p_{hx}p_{hy}\{J_x,J_y\}+\text{c.p.}), \tag{5}$$

where $\mathbf{p}_{e,h}$ are the electron and hole momentum operators $-i\hbar\nabla_{e,h}$, J is a spin-3/2 angular momentum operator, m_0 is the free-electron mass, m_c is the conduction-band mass, γ_1, γ_2, and γ_3 are the Luttinger parameters, $\{a,b\}\equiv(1/2)(ab+ba)$, and c.p. stands for cyclic permutations. ε is the dielectric constant, and ε_f is the permittivity of free space. The conserved total exciton momentum is $\mathbf{P}_T=\mathbf{p}_e+\mathbf{p}_h$ with eigenvalues $\hbar\mathbf{K}$. In Kane's perturbation theory[14] the terms that involve γ_2 and γ_3, the "d-like" part of $H_{e\text{-}h}$, are treated as a perturbation on the "s-like" part of $H_{e\text{-}h}$ which has a hydrogenlike spectrum. In second order the energy shift of the $1s$ state from the conduction-band minimum is given by

$$E_{1s}(\mathbf{K})=-EB_{1s}+\Delta E(\mathbf{K})$$
$$=-EB_{1s}+\frac{\hbar^2K^2}{2m_0}\{A\mp[B^2+C^2g(\vartheta,\phi)]^{1/2}\},$$
$$g(\theta,\phi)=\tfrac{1}{4}(\sin^4\vartheta\sin^2 2\phi+\sin^2 2\vartheta), \tag{6}$$

where EB_{1s} is the binding energy and we have used polar coordinates K,ϑ,ϕ. The constants A, B, and C are expressed through m_c, γ_1, γ_2, and γ_3 (Ref. 14) and $C\neq 0$ if $\gamma_2\neq\gamma_3$. The two signs in Eq. (6) give heavy and light excitons. Although the light exciton dispersion is only slightly anisotropic, the heavy-exciton dispersion is strongly anisotropic. If one defines an effective direction dependent mass $M(\hat{\mathbf{K}})$, given by the inverse curvature of $E(\mathbf{K})$ at $K=0$, and uses parameter values from Table I, then for different directions in reciprocal space one obtains for the heavy exciton in GaAs $M\langle 100\rangle=0.8$, $M\langle 110\rangle=1.5$, and $M\langle 111\rangle=2$.

For the evaluation of the exciton-phonon interaction matrix elements, we will use a spherical model approximation for the exciton wave functions.[20,21] The spherical model is obtained from Eq. (5) by replacing γ_2 and γ_3 by one parameter γ:

$$H_{\rm SP}=\frac{p_e^2}{2m_c}+\frac{p_h^2}{2m_0}\left(\gamma_1+\frac{5}{2}\gamma_2\right)-\frac{\gamma}{m_0}(\mathbf{p}_h\cdot\mathbf{J})^2$$
$$-\frac{e^2}{4\pi\varepsilon\varepsilon_f|\mathbf{r}_e-\mathbf{r}_h|}. \tag{7}$$

The value of γ in Ref. 21 was used giving $\gamma=(2\gamma_2+3\gamma_3)/5$ as the one that results in a reasonable approximation for the binding energy of an exciton at rest.

In the simple band model, the relative motion of the electron and hole can be separated from the COM motion by a linear coordinate transformation. There is no such transformation for the Hamiltonian in Eq. (7). One can still define a relative electron-hole wave vector by

$$\mathbf{k}_e=\alpha_e\mathbf{K}+\mathbf{k},\quad \mathbf{k}_h=\alpha_h\mathbf{K}-\mathbf{k}, \tag{8}$$

with arbitrary coefficients satisfying $\alpha_e+\alpha_h=1$. The eigenfunctions of $H_{e\text{-}h}$ can be written as

$$\Phi_{\rm ex}^{(\mathbf{K})}(\mathbf{r}_e,\mathbf{r}_h)=e^{i\mathbf{K}\cdot\mathbf{R}}\Phi^{(\mathbf{K})}(\mathbf{r}), \tag{9}$$

where $\mathbf{R}=\alpha_e\mathbf{r}_e+\alpha_h\mathbf{r}_h$ and $\mathbf{r}=\mathbf{r}_e-\mathbf{r}_h$. The functions $\Phi(\mathbf{r})$ are obtained as eigenfunctions of the $\mathbf{K}$-dependent effective Hamiltonian.[15] The total angular momentum can be written as $\mathbf{J}_{\rm tot}=\mathbf{F}+\mathbf{s}=\mathbf{L}+\mathbf{J}+\mathbf{s}$, where $\mathbf{J}$ and $\mathbf{s}$ are spin-3/2 and -1/2 operators of hole and electron, respectively, and $\mathbf{L}$ is the orbital angular momentum of the exciton. We will use the notation M, μ, and ν for the projections of $\mathbf{F}$, $\mathbf{J}$, and $\mathbf{s}$. We choose $\hat{\mathbf{K}}$ as the direction of quantization for angular momenta. $\mathbf{F}$ is not conserved even in the spherical model, but $M\equiv F_z$ is conserved. Using the L-J coupling scheme,[15,17] the exciton eigenstates can be written as

$$\Phi_{\lambda;M,\nu}^{(K)}(\mathbf{r})=\sum_{\mu}\phi_{\lambda;M,\nu,\mu}^{(\mathbf{K})}(\mathbf{r})$$
$$=\sum_{L,F}R_{\lambda;L,F}^{(\mathbf{K})}(r)|L,J=3/2,F,M,\nu\rangle, \tag{10}$$

where

$$|L,J,F,M,\nu\rangle=(2F+1)^{1/2}(-1)^{L-J+M}$$
$$\times\sum_{m+\mu=M}\begin{pmatrix}L & J & F\\ m & \mu & -M\end{pmatrix}Y_{Lm}(\vartheta,\phi)u_\mu^z v_\nu^z, \tag{11}$$

u_μ and v_ν are the hole and electron spinor functions, $\mu=\pm 1/2,\ \pm 3/2$, $\nu=\pm 1/2$, the index γ denotes the bound exciton states analogous to the hydrogenic states of the simple band model, and we use the $3j$ symbols defined in the theory of addition of angular momenta.[11]

The study of the K-dependent Hamiltonian obtained as a result of the coordinate transformation in Eq. (8) is greatly facilitated by expressing $\mathbf{p}$ and $\mathbf{J}$ operators in terms of irreducible spherical tensors. The corresponding expressions and selection rules can be found in Refs. 15 and 17. The matrix elements of the tensor products can be evaluated using the Wigner-Eckart theorem and $6j$ symbols.[22,23] The exciton Hamiltonian is given in terms of spherical tensor operators in Appendix A.

At $K=0$ the exciton problem is formally similar to the shallow acceptor problem,[24–26] and the ground state, which we denote by $\lambda=1s$, can be written as

$$\Phi^{(0)}_{1s;3/2,M,\nu}(\mathbf{r}) = R_0(r)|0,3/2,3/2,M,\nu\rangle + R_2(r)|2,3/2,3/2,M,\nu\rangle. \quad (12)$$

R_0 and R_2 are found as solutions of the system of two coupled differential equations. Because of the coupling, the behavior of $R_2(r)$ near the origin is different from that in a hydrogenic model. We choose a variational treatment of the problem,[24] with

$$R_0(r) = A\alpha^{3/2}e^{-\alpha r}, \quad R_2(r) = B\beta^{5/2}re^{-\beta r}, \quad (13)$$

which reproduces the correct r dependence at small r, found by a polynomial expansion of the radial functions. We find that R_2 is much smaller than R_0 and define an effective exciton radius as $a_{\rm exc}=1/\alpha$. The values of $a_{\rm exc}$ obtained in the spherical model are given in Table I. At $K\neq 0$ there are infinitely many terms in the expansion in Eq. (10). Following Ref. 15, we consider only those basis states that are coupled to the $L=0$ state in first order. This restriction can be shown to reduce the exciton problem to a four-dimensional subspace for the $M=\pm 3/2$ case and a five-dimensional subspace for the $M=\pm 1/2$ case. A particular choice of the linear transformation coefficients in Eq. (8) eliminates the coupling of the $L=0$ state to the $|1,3/2,3/2,M,\nu\rangle$ states. Defining $\gamma_e \equiv 1/m_c$, this choice can be shown to be

$$\alpha_h = \frac{\gamma_e}{\gamma_e+\gamma_1-4\gamma/\sqrt{3}}, \quad (14)$$

with $\alpha_e = 1-\alpha_h$. Consider the $M=\pm 3/2$ case. Using a variational function $R_{1,5/2}(r) = iC\eta r\exp(-\eta r)$, one can show that the coupling of the $L=0$ state to the $|1,3/2,5/2, \pm 3/2,\nu\rangle$ state is small unless K is large. For example, in the GaAs case with this choice of α_e and α_h, the coupling of the $L=0$ state to this state is smaller than the coupling to the $L=2$ state by a factor of $0.13(Ka_{\rm exc})^2$, where $a_{\rm exc}$ is the radius of the $L=0$ state given in Table I. It is then justified to neglect this coupling for small and intermediate ($K \sim 1/a_{\rm exc}$) values of exciton total momenta. We can therefore estimate the exciton form factors for the $1s$ state by using the $L=0$ wave function and α_e, α_h from Eq. (14).

III. EXCITON INTERACTION WITH ACOUSTIC PHONONS IN BULK SEMICONDUCTORS

Because we will include multiple-phonon processes in our calculation, it is convenient to use second quantization, with $\hat{B}$ and $\hat{a}$ standing for exciton and phonon annihilation operators. The exciton-phonon interaction Hamiltonian is given by

$$H_{\text{exc-phon}} = \sum V_{\lambda\lambda';MM';\nu\nu';\tau}(\mathbf{K},\mathbf{K}')\hat{B}^{\dagger}_{\lambda' M'\nu'}(\mathbf{K}')\hat{B}_{\lambda M\nu}(\mathbf{K}) \times(\hat{a}_{\mathbf{K}'-\mathbf{K},\tau}+\hat{a}^{\dagger}_{\mathbf{K}-\mathbf{K}',\tau}), \quad (15)$$

where τ denotes three phonon polarization states. In the complex band model, in which the degeneracy of the valence band is taken into account, the matrix element V depends on both the initial and final momenta.

If we consider an exciton in its ground state to be created by a circularly right-polarized photon with momentum $\hbar\mathbf{K}_{\rm phot}$, then $M+\nu=1$ with the quantization axis along $\mathbf{K}_{\rm phot}$. The electron spin is not changed in the scattering, and we will drop the ν index. Because the photon wave vector at optical frequencies is small, in the evaluation of phonon induced exciton linewidth by FGR we can set the initial momentum of the exciton to be zero. If we consider for the moment only the $1s$ exciton states and use just the $L=0$ part as an approximation for the wave function, the corresponding exciton-phonon matrix element for DP interaction can be shown to be

$$V^{\rm DP}_{M,M';\tau}(0,\mathbf{q}) = \sum_{\mu} D^{*}_{M'\mu}(\vartheta',\varphi') \times \int d^3k[U^{c}_{\tau}(q)\phi_0(\mathbf{k})\phi_0(\mathbf{k}+\alpha_h\mathbf{q}) - U^{v}_{M\mu;\tau}(-\mathbf{k},-\mathbf{k}+\mathbf{q})\phi_0(\mathbf{k})\phi_0(\mathbf{k}-\alpha_e\mathbf{q})], \quad (16)$$

where ϑ' and φ' are the polar angles of the vector $\mathbf{q}$ with respect to the quantization axis z, $\phi_0(k)$ is the Fourier transformation of $R_0(r)/\sqrt{4\pi}$, and the 4×4 matrix $D_{mn}(\vartheta,\varphi) = \exp(\text{i}m\phi)d_{mn}(\vartheta)$ is the spin-3/2 representation of the rotation group.[11] The momentum-dependent coefficients U^c and U^v are the interaction matrix elements for the electron-phonon and hole-phonon scatterings, respectively.

For a simple isotropic conduction band the deformation potential is a scalar[13] and the corresponding matrix element is

$$U^{c}(q) = iV^{-1/2}\left(\frac{\hbar q}{2\rho v_{\rm LA}}\right)^{1/2} D_c, \quad (17)$$

where V is the volume and D_c is the conduction-band (scalar) deformation potential. The deformation potential operator w_{nm} that enters into the hole–acoustic-phonon interaction[13,27] is given by a convolution of the second-rank operator tensor Ξ^{ij}_{nm} with the strain tensor u_{ij} where the indices i,j refer to the coordinate components x, y, z and n, m refer to the components of a 4×4 matrix in the $J=3/2$ subspace: $w_{nm} = \Xi^{ij}_{nm}u_{ij}$, with

$$\Xi^{xx} = \left(a+\frac{5}{4}b\right)I - bJ_x^2, \quad \Xi^{xy} = -\frac{d}{\sqrt{3}}\{J_x,J_y\}, \quad (18)$$

where I is the identity operator and the other components are obtained by cyclic permutations. In the spherical model the isotropic form of the deformation potential is obtained by defining b as $d/\sqrt{3}$.[28]

The values of deformation potential constants along with other material parameters used here are listed in Table II. The coefficients $U^{v}_{\mu\mu';\tau}$ are obtained from the parameter tensor Ξ and the four eigenvectors of the valence band Hamiltonian in Eq. (5) in the following way.[13] Define the following convolution matrix:

TABLE II. Values of material parameters in the electron-phonon interaction and calculated values of the linear coefficient in the temperature dependence of the acoustic-phonon-induced HWHM of the exciton.

	ε	ρ (g/cm^2)	v_{LA} (10^5 cm/s)	v_{TA} (10^5 cm/s)	D_c (eV)	a (eV)	b (eV)	e_{14} (C/m^2)	d_{ac} (μeV/K)
GaAs	12.5[b]	5.3[c]	4.8[c]	3.34[c]	-9.3[d]	2.7[c]	-2.62	0.16[f]	7.8
ZnSe	8.8[a]	5.65[e]	4.2	2.7	-8[h]	-2[h]	-1	0.049[g]	9.6

[a]Reference 43.
[b]Reference 14.
[c]Reference 32.
[d]Reference 33.
[e]Reference 44.
[f]Reference 45.
[g]Reference 46.
[h]An estimate deduced from the papers in Ref. 47.

$$[\Xi_{\tau\mathbf{q}}]_{nm} = \tfrac{1}{2}\,\Xi^{ij}_{nm}(d_{i,\tau\mathbf{q}}e_j + d_{j,\tau\mathbf{q}}e_i), \tag{19}$$

where $\mathbf{d}_{\tau\mathbf{q}}$ is a dimensionless phonon polarization vector and $\mathbf{e}\equiv\mathbf{q}/q$. Consider the eigenvectors of H_v in the $J=3/2$ subspace, $A_l(\mathbf{k})$, with components $A_{ln}(\mathbf{k})$ with l and $n=\pm 3/2$, $\pm 1/2$. These components enter the expansion of the Bloch functions at the degeneracy point $\mathbf{k}_0$: $u_{l\mathbf{k}}(\mathbf{r}) = \Sigma_n A_{ln}(\mathbf{k}) u_{l\mathbf{k}_0}(\mathbf{r})$. Using a tensor product of A_l's, we define the 4×4 matrices

$$[A^{ll'}(\mathbf{k},\mathbf{k}')]_{nn'} \equiv A_{ln}(\mathbf{k}) A^*_{l'n'}(\mathbf{k}') \tag{20}$$

and define the deformation potentials $\Theta^{ll'}$ by the trace operation in the $J=3/2$ subspace:

$$\Theta^{ll'}_{\tau\mathbf{q}}(\mathbf{k},\mathbf{k}') \equiv \mathrm{tr}(A^{ll'}\Xi_{\tau\mathbf{q}}). \tag{21}$$

Using these potentials, the hole-phonon interaction elements in Eq. (16) are found as

$$U^{v}_{ll';\tau}(-\mathbf{k},-\mathbf{k}+\mathbf{q}) = iV^{-1/2}\left(\frac{\hbar q}{2\rho v_{\mathrm{LA}}}\right)^{1/2}\Theta^{ll'}_{\tau\mathbf{q}}(-\mathbf{k},-\mathbf{k}+\mathbf{q}). \tag{22}$$

The exciton-phonon matrix element for the piezoelectric interaction can be shown to be

$$V^{\mathrm{PE}}_{M,M';\tau}(0,\mathbf{q}) = \sum_{\mu} D^*_{M'\mu}(\vartheta',\varphi') \times \int d^3k\, U^{\mathrm{PE}}_{\tau}(\mathbf{q})[\phi_0(\mathbf{k})\phi_0(\mathbf{k}+\alpha_h\mathbf{q}) - \phi_0(\mathbf{k})\phi_0(\mathbf{k}-\alpha_e\mathbf{q})], \tag{23}$$

with the electron-phonon matrix element U^{PE} is given by

$$U^{\mathrm{PE}}_{\tau}(q) = \frac{2ee_{14}}{\bar{\varepsilon}q^2}\left[\frac{\hbar}{2\rho\omega_\tau(q)V}\right]^{1/2}(q_xq_yd_{z,\tau q} + \mathrm{c.p.}), \tag{24}$$

where $\omega_\tau(\mathbf{q})$ is phonon frequency for a given polarization τ. Also, $\bar{\varepsilon}\equiv\varepsilon\varepsilon_f$ with ε_f being the permittivity of vacuum, 8.854×10^{-12} F/m.

The phonon-induced linewidth of the exciton state ($\lambda = 1s, K\approx 0, M, \nu$) defined in Eq. (10) can be evaluated in the one-phonon processes approximation using FGR. It is then a linewidth resulting from the scatterings to the final exciton states ($\lambda = 1s, \mathbf{K}=\mathbf{q}, M', \nu$) with $M'=\pm 3/2$, $\pm 1/2$, and taking thermal average over the phonon population, we obtain

$$\Gamma^{\mathrm{FGR}}_{1s,M} = \Gamma^{\mathrm{DP}}_{1s,M} + \Gamma^{\mathrm{PE}}_{1s,M},$$

$$\Gamma^{u}_{1s,M} = \pi\int d^3q\,\frac{V}{(2\pi)^3}\sum_{M',\tau}\frac{k_BT}{\hbar v_\tau q}|V^{u}_{MM';\tau}(0,\mathbf{q})|^2 \times \delta(\Delta E_{M'}(\mathbf{q}) - \hbar v_\tau q), \tag{25}$$

where for ΔE we use an anisotropic dispersion obtained in Eq. (6) and the index u stands for DP and PE. If the $1s$ exciton wave function is approximated by its $L=0$ part, as implied in Eq. (16), the TA phonons do not contribute to DP scattering at this level of approximation.

Using the parameters from Tables I and II, we obtain the scattering rates and corresponding linewidths for the two states that can be created by a circularly polarized photon, ($M=3/2, \nu=-1/2$) and ($M=1/2, \nu=1/2$). In the absence of exciton-phonon interactions these states are degenerate at $K=0$, but the degeneracy is slightly split by the interaction, the splitting given by the difference of the real parts of the corresponding self-energies. The imaginary parts of the self-energy in the FGR approximation are the linewidths in Eq. (25). They are slightly different for the two states, the difference being much smaller than either of $\Gamma_{1s,3/2}$ and $\Gamma_{1s,1/2}$. The corresponding optical linewidth then will be given by the larger of two. The results for the HWHM are $\Gamma^{\mathrm{FGR}}/k_BT = 7.80\,\mu$eV/K for bulk GaAs and 9.58 μeV/K for bulk ZnSe. These values are quite close to the experimental HWHM linewidths in bulk GaAs,[5,29,30] 8–10 μeV/K, and bulk ZnSe,[31] 10 μeV/K. These experimental results were obtained by resonant Raman scattering,[3] optical dephasing,[29] and photoluminescence.[30,31] They are also much larger than the values obtained in the simple band theory[7,8] with the exciton form factors given by Eqs. (2) and (3). In the case of bulk GaAs we find that the dominant contribution to the scattering rate, about 85%, comes from the PE interaction and only 15% comes from the DP interaction. Within the DP contribution, the dominant part comes from the conduction-

band electron scattering. Therefore, the total result will not be sensitive to the factor-of-2 variations of valence-band deformation potential values for GaAs that one encounters in the literature.[32,33]

In the case of bulk ZnSe, on the other hand, almost all the contribution comes from the DP interaction, with the PE interaction contributing less than 1%. The reason for the large PE contribution in bulk GaAs was indicated earlier following Eq. (4). For ZnSe, on the other hand, there are two factors contributing to the negligible PE effect on the exciton: the value of e_{14}^2 is much smaller than in GaAs, and the small effective exciton size, represented by $a_{\rm exc}$ in Table I, greatly diminishes the exciton form factor for the PE interaction. In addition, we find that the smallness of the exciton size makes the exciton form factor for ZnSe dependent more on the difference of the DP parameters for the conduction and valence bands, $|D_c - a|$, rather than on their values separately. This is useful to know because the differences between band deformation potentials are easier to determine than the potentials.

IV. EFFECTS OF MULTIPLE-PHONON SCATTERINGS IN BULK EXCITON ABSORPTION

To go beyond the FGR approximation, we turn now to the contribution of the multiple-phonon processes to the exciton linewidth. These have been evaluated by Toyozawa[34] for the DP interaction in the simple band model using a quasielastic approximation for acoustic phonons and neglecting the momentum dependence of the exciton form factor. That last approximation required the use of the sharp cutoff at large values of momentum transfer. In Ref. 34 the Debye wave vector was chosen somewhat arbitrarily as the cutoff. As the result of the elastic phonon approximation (EPA) in the renormalized exciton propagator, the absorption line shape near the band edge was obtained in the temperature-independent form of $f(E/k_B^2T^2)$, with the linewidth$\propto T^2$. In the EPA the $\Gamma^{\rm FGR}=0$, and the nonzero result at the unrenormalized exciton-phonon vertex level of approximation comes from the self-consistent type of diagrams in the standard perturbation theory[12,35]—i.e., the diagrams in which the virtual phonons are reabsorbed (reemitted) in the order opposite to their emission (absorption).

In Toyozawa's formalism, the sum of all such terms corresponds to a lowest-order approximation in the exciton-phonon interaction for the thermal average of the exciton resolvent operator.[34] The criterion for the self-consistency of the approximations used in Ref. 34 as applied to the DP interaction in GaAs requires $T>70$ K. It seems to us, however, that the criterion for the validity of the EPA is $\Gamma^{\rm SC}>\Gamma^{\rm FGR}$, where $\Gamma^{\rm SC}$ is the linewidth evaluated in the self-consistent approximation with the EPA and $\Gamma^{\rm FGR}$ is the FGR result for the DP interaction. From this criterion we deduce the requirement $T>270$ K in the case of GaAs. Thus the T^2 dependence of the linewidth obtained in Ref. 34 will not be observed at temperatures where the exciton–acoustic-phonon scattering dominates the temperature dependence.

We start by outlining a multiple-phonon theory based on the Hamiltonian in Eq. (15) in the one-exciton subspace. Unlike in the FGR approximation, both (virtual) phonon emission and absorption contribute to the exciton self-energy, as do exciton states other than $1s$. We find, however, that at least in the simple band model the scatterings to the p state and higher excited states make negligible contributions to the linewidths of the $1s$ state and restrict the formalism to the $1s$ exciton subspace. The time-dependent exciton propagator is defined as[12]

$$G_{nn'}(\mathbf{K},t) = -i\,\theta(t)\langle\langle B_n(\mathbf{K},t)B_{n'}^{+}(\mathbf{K},0)\rangle\rangle, \tag{26}$$

where index n refers to the quantum numbers M and ν that define an exciton state, all operators are in the Heisenberg picture, and the double brackets imply a thermal average over the phonon ensemble. The electron spin projection is not affected by the electron-phonon scattering and will not be referred to explicitly here. Because of the degeneracy of the $\pm M$ exciton states at any $\mathbf{K}$,[15] one can formulate the theory in such a way that the index n is two valued, referring to the ''heavy''- and ''light''-exciton branches, which we will denote as $n=1$ and $n=2$, correspondingly. The frequency-dependent $G_{nn'}(\mathbf{K},\omega)$ is defined as a Fourier transformation over time, and we write the 2×2 propagator matrix as $\hat{G}(\mathbf{K},\omega)$. The noninteracting propagator will be denoted as $\hat{G}^0(\mathbf{K},\omega)$, and Dyson's equation for the propagator is

$$\hat{G} = \hat{G}^0 + \hat{G}^0\hat{\Sigma}\hat{G}, \tag{27}$$

where the self-energy $\hat{\Sigma}(\mathbf{K},\omega)$ is also a 2×2 matrix. One can then obtain a perturbation expansion for the exciton self-energy in a standard way.[12]

Let the exciton-photon interaction matrix element for an exciton in state n and a photon with wave vector k and polarization ξ be $T(\xi,\mathbf{k},n)$. The probability of one-photon absorption is found as[12]

$$\frac{1}{\tau_{\mathbf{k}\xi}} = -2\sum_{n,n'} T(\xi,\mathbf{k},n)T^*(\xi,\mathbf{k},n')\,\mathrm{Im}\,G_{nn'}(\mathbf{k},\omega). \tag{28}$$

For a weak exciton-phonon interaction, the off-diagonal elements of $\hat{\Sigma}$ can be neglected compared to the diagonal ones, and then the absorption line shape is obtained from Eq. (28), setting $k_{\rm phot}=0$:

$$\alpha(\omega) = -\sum_{n=1,2}\frac{\Sigma''_{nn}(\omega)}{[\hbar\omega - E_{1s} - \Sigma'_{nn}(\omega)]^2 + [\Sigma''_{nn}(\omega)]^2}, \tag{29}$$

where Σ' and Σ'' are the real and imaginary parts of the self-energy, and E_{1s} is the energy of the exciton state in the absence of the interaction. At the FGR level of approximation one obtains a sum of two Lorentzians, with $|\Sigma'_{11}-\Sigma'_{22}|$ small compared to Σ'_{11}.

Rather than proceed with explicitly including the anisotropy of the valence band in the exciton propagator, we will take here a simpler approach of an effective simple band model in the estimating the effects of the multiple-phonon processes on the optical linewidth. In this approach we will

replace the valence-band DP interaction matrix element $U^{\nu}_{M,\mu;\tau}(-\mathbf{k},-\mathbf{k}+\mathbf{q})$ in Eq. (16) by an effective scalar deformation potential

$$U^{\nu,\mathrm{eff}}_{M}(q)=iV^{-1/2}\left(\frac{\hbar q}{2\rho v_{\mathrm{LA}}}\right)^{1/2}D^{\mathrm{eff}}_{\nu}, \tag{30}$$

with D^{eff}_{ν} defined using an angular average of $U^{\nu}_{M,M';\tau}(0,\mathbf{q})$ which is also averaged over two $\pm|M'|$ values with respect to the second index. We will also define the effective simple band exciton mass by equating the resulting FGR scattering rate to the corresponding result of the complex band model in the previous section. This mass will depend on interaction strengths of both DP and PE interactions. Using the parameter values in Tables I and II, we obtain, for GaAs, $D^{\mathrm{eff}}_{\nu}\approx 1.46$ eV, $M^{\mathrm{eff}}/m_0\approx 1.71$.

We can also include the effect of the impurity scattering on the exciton self-energy. In doing so we will neglect the real part of the impurity-induced energy shift of the exciton energy and denote the frequency-independent imaginary part by $\Gamma(0)$. This $\Gamma(0)$ corresponds to the temperature-independent part of the exciton linewidth in Eq. (1) that we would obtain if we had used the FGR approximation. The summation of the self-consistent terms gives an equation for the part of the self-energy, which we refer to as $\Sigma^{(2)}$, and neglecting the dependence of Σ on momentum variations, we use an approximation that gives a correct FGR limit:

$$\Sigma^{(2)}(\omega)=\int d^3q\,\frac{V}{(2\pi)^3}\,2\sum_{\tau}\,[|V^{\mathrm{DP}}_{\tau}(q)|+|V^{\mathrm{PE}}_{\tau}(q)|^2]\times\left[\frac{N_{\tau}(\mathbf{q})}{\hbar\omega+\hbar\omega_{\tau}(\mathbf{q})-E_{\mathrm{exc}}(\mathbf{k}+\mathbf{q})-\Sigma^{(2)}(\omega)+i\Gamma(0)}+\frac{N_{\tau}(\mathbf{q})+1}{\hbar\omega-\hbar\omega_{\tau}(\mathbf{q})-E_{\mathrm{exc}}(\mathbf{k}-\mathbf{q})-\Sigma^{(2)}(\omega)+i\Gamma(0)}\right], \tag{31}$$

where $N_{\tau}(\mathbf{q})$ is the acoustic phonon occupation at a given temperature and $\omega_{\tau}(\mathbf{q})$ and $E_{\mathrm{exc}}(\mathbf{k})$ are the phonon and exciton dispersions, respectively. The factor of 2 comes from the summation over the two degenerate values of the final-state exciton quantum number M'. At temperatures above 10 K we can replace $N(q)$ by $k_BT/\hbar qv_{\tau}$ and neglect the spontaneous-phonon emission term. The absorption line shape in the self-consistent approximation is then found by numerical solution of Eq. (31) and using Eq. (29).

As we know from Toyozawa's work,[34] the vertex terms in the perturbation theory for the self-energy can make a significant contribution to the total absorption. We will consider the same two classes of the self-energy vertex diagrams as in Ref. 34 in the partial summation of the vertex corrections. From the point of view of the corrections to the exciton-phonon interaction vertex,[12] these terms fall in two classes: ladder diagrams and maximally crossed diagrams in terms of phonon lines. Here, however, we do not need a momentum cutoff, the convergence of the integrals being provided by the wave vector dependence of the exciton form factors in Eqs. (2) and (3). These terms can be summed up with some additional approximations, as explained in Appendix B. Each term of the order $2n$ in the exciton-phonon interaction carries a factor proportional to T^{2n}. The resulting equation for $\Sigma=\Sigma^{(2)}+\Sigma^{(4)}+\Sigma^{(6)}+\cdots$ looks like Eq. (31) with a renormalized frequency-dependent interaction vertex. The solution of this transcendental equation was then performed numerically.

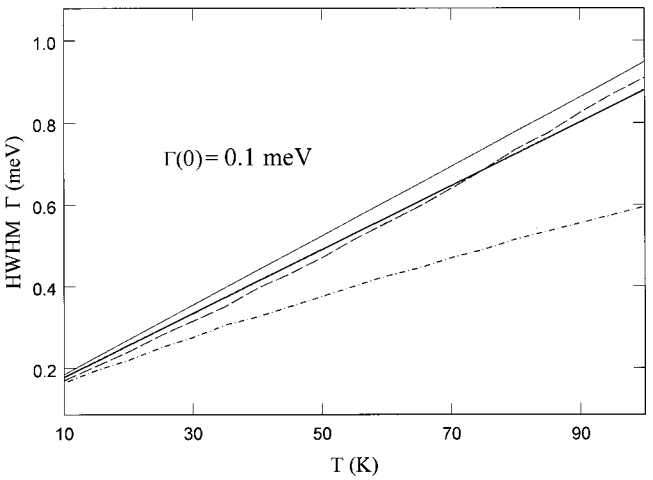

FIG. 1. Linewidth $\Gamma(T)$, defined as the HWHM, for bulk GaAs shown for $\Gamma(0)=0.1$ meV as a function of temperature. The thick solid line shows the FGR approximation in the complex band model, Eqs. (1) and (25). The dashed line shows $\Gamma(T)$ with multiple-phonon contributions including the vertex terms. The dash-dotted line shows $\Gamma(T)$ with only self-consistent terms $\Sigma^{(2)}$. It is seen that the vertex terms mostly cancel the self-consistent corrections to the linewidth. The thin solid line shows the linewidth of the corresponding transverse exciton-polariton calculated in the FGR approximation.

The optical exciton linewidth defined as the HWHM was found from the absorption line shape $\alpha(\omega)$. The results for bulk GaAs are shown in Fig. 1 for $\Gamma(0)=0.1$ meV, as functions of temperature in the 10–100 K range. The thick solid line shows the FGR approximation in the complex band model, Eqs. (1) and (25). The dashed line shows $\Gamma(T)$ with the inclusion of the multiple-phonon contributions, including the vertex terms. The dash-dotted line shows $\Gamma(T)$ with only self-consistent terms $\Sigma^{(2)}$ included. It is seen in Fig. 1 that the vertex terms mostly cancel the self-consistent corrections to the linewidth, the resulting linewidth being approximately linear in T. The thin solid line shows the linewidth of the corresponding transverse exciton polariton, calculated in the FGR approximation, including both phonon absorption and emission[36] and using the effective simple band model with the same parameters as we obtained for the exciton problem. The transverse polariton linewidth in bulk GaAs is thus found to be quite close to the exciton linewidth.

From Fig. 1 we conclude that the inclusion of the multiphonon processes has only a small effect on the exciton linewidths in GaAs, as compared to the FGR result. At higher temperatures multiphonon processes modify the shape of the absorption curve without affecting the linewidths. In Fig. 2 we show the absorption line shapes for three different values of the temperature, 20, 50, and 100 K with the same

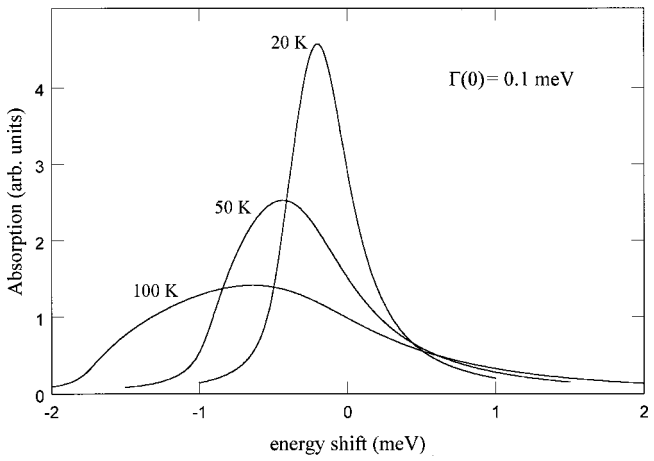

FIG. 2. Absorption line shapes for three different values of temperature, 20, 50, and 100 K, with the same value of $\Gamma(0)=0.1$ meV as in Fig. 1. With an increase of temperature the line shape becomes asymmetric.

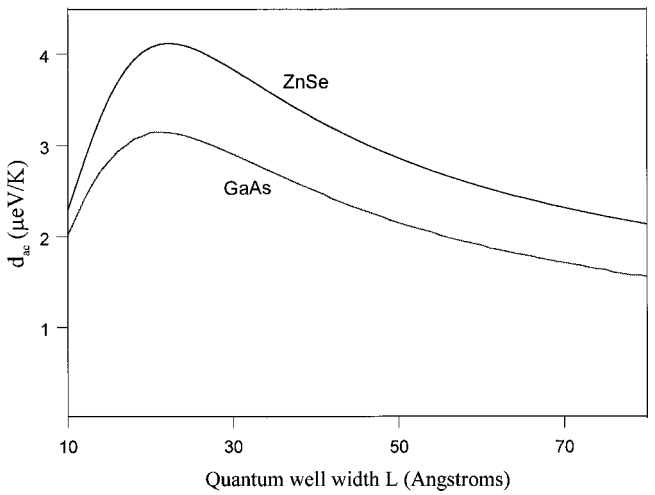

FIG. 3. Linear coefficient $d_{\rm ac}$ in the temperature dependence of the linewidth $\Gamma(T)$, defined as the HWHM, is shown as a function of the well width for GaAs/$Al_{0.2}Ga_{0.8}$As and ZnSe/ZnMgSSe quantum wells.

value of $\Gamma(0)$ as in Fig. 1. We see that at higher temperatures the line shape becomes asymmetric. If we neglect the impurity scattering and set $\Gamma(0)$ to zero, every absorption curve will have a sharp edge at the lower frequencies.[34] We find that with increasing value of the impurity scattering the low-energy edge broadens and the line shapes become more symmetric. Therefore, only in a very pure material could the multiphonon modification of the optical exciton line shape be observed.

In each order of interaction, most of the contribution comes from scattering to the ''heavy-exciton'' branch in Eq. (6), with scattering to the ''light-exciton'' branch contributing little. Also, scattering to the exciton states other than the $1s$ state was found to be negligible. In addition, we evaluated the effect of the exciton-phonon interaction vertex renormalization by the effect of the moving impurities—i.e. the motion of impurities in the phonon field.[37] This effect is known to be of importance in the microscopic theory of sound attenuation in impure metals.[38] In the case of semiconductors the motion of impurities could lead to a temperature-dependent contribution to the exciton linewidth and this effect is evaluated in Appendix C. To leading order in the effective ''three-body'' exciton-impurity–phonon interaction the effect on the linewidth is found to be negligible. The details are given in Appendix C.

V. EXCITON–ACOUSTIC-PHONON SCATTERING IN SEMICONDUCTOR QUANTUM WELLS

Turning next to exciton–acoustic-phonon scattering in semiconductor quantum wells, we notice that the symmetry is lowered and the degeneracy of the valence band at the zone center is partially lifted. The effective exciton Hamiltonian is then is more complicated than in the bulk case, and an evaluation of the scattering rates in the complex band model for the wide wells requires a large set of basis functions to describe the exciton wave function. The picture is simpler for the narrower wells where the large splitting of the heavy- and light-hole branches allows one to use a simple band model for heavy holes, at least at small wave vectors. We then proceed with a simple effective-mass band model similar to that used in our earlier investigation of the exciton–LO-phonon scattering rates.[39]

Consider a GaAs/Al_xGa_{1-x}As well with isotropic conduction band with the effective mass in the well, $m_{\rm cw}=0.067m_0$, and mass in the barriers, $m_{\rm cb}=(0.067+0.835x)m_0$. For the heavy holes we use the in-plane mass $m''_{hhw}=0.18m_0$,[39] the mass for the growth direction $m'_{hhw}=0.34$ in the well, and $m_{hhb}=(0.34+0.42x)m_0$. From the known band alignments we find the barrier heights for the electrons and holes, $V_c=0.8355x$ eV and $V_v=0.4115x$ eV. The dependence of the band parameters on the A1 concentration x was obtained from Ref. 40. The tunneling of the carriers into the barriers was taken into account in the exciton form factor by the use of effective well widths,[40] obtained by equating the normalization constants of the finite- and infinite-barrier models. We consider first the FGR approximation for the exciton-phonon scattering rates. Here, unlike the case of bulk GaAs, the contribution of PE interactions was found to be negligible as compared to the contribution of DP interactions. This is due to the effect of the nearly complete decoupling of the light and heavy holes in narrow quantum wells on the exciton form factor.

The resulting linewidth, defined as the HWHM of the absorption spectrum, depends linearly on temperature, and the linear coefficient $d_{\rm ac}$ is shown in Fig. 3 as a function of the well width, for $x=0.2$. The overall magnitude of $d_{\rm ac}\sim 2-3$ μeV/K is in generally good agreement with experimental results for quantum wells,[1,3,4,5] 1–3 μeV/K, obtained using transmission,[1] resonant Raman scattering,[3] optical dephasing,[4] and photoluminescence.[5] The results in Fig. 3 are for relatively narrow wells in which excitons in only the first electron and hole subbands contribute. For wider wells, this contribution decreases due to the normalization factor of the subband functions. As the well becomes wider, there would be an increase in $d_{\rm ac}$ over the values in Fig. 3 as more

subbands become accessible as final states. Eventually, as the quantum well becomes wide enough, the subbands collapse on together, and the result should go over to the bulk values for d_{ac} given in Table II.

In Fig. 3 we also give results for quantum wells of ZnSe with ZnMgSSe barriers, systems that have been of experimental interest recently. The material parameters for these systems are given in Ref. 41. The overall magnitudes obtained here ($d_{ac} \sim 4\ \mu$eV/K) are compatible with available experimental estimates of $d_{ac} \sim 5-10\ \mu$eV/K.[31,41] The material parameters for these structures are less well known than in the case of GaAs/AlGaAs structures.

In order to estimate the effect of the self-consistent multiphonon terms in the two-dimensional (2D) limit we have evaluated $\Sigma^{(2)}$ in the 2D version of Eq. (31) and found that the results for the linewidths are close to those obtained with the FGR approximation. An evaluation of the vertex terms in 2D turns out to be more complicated than in bulk, but we do not expect them to contribute significantly more than the self-consistent terms. In fact, there is a general argument due to Toyozawa, that the multiphonon terms in 2D are small:[42] because the density of states near the exciton band edge in the 2D system does not vary as sharply as in bulk system, the effects of the scattering to the intermediate states on the exciton propagator should be significantly less than in bulk. That is what we found in the evaluation of the self-consistent corrections in 2D, and a similar result is expected for the vertex corrections. Therefore, the values of the exciton linewidth in narrow wells obtained with the FGR approximation and shown in Fig. 3 should be reasonably accurate.

VI. SUMMARY AND DISCUSSION

In the present work we have evaluated the optical absorption spectra and the contribution of acoustic phonons to the exciton linewidths in bulk and narrow quantum wells of direct band-gap cubic semiconductors, with numerical results given for GaAs and ZnSe. Experimental results have shown that the acoustic phonon contribution to the homogeneous exciton linewidth increases substantially in going from quantum wells to bulk. In prior theoretical work the exciton-phonon interaction effects in optical spectra have been treated using a simple band model in which the valence band is replaced by a single parabolic band with heavy-hole mass. Perturbation theory for acoustic phonon scattering using the deformation potential interaction and isotropic dispersion of a simple band description accounts for experiment in quantum wells, but it fails by an order of magnitude for bulk GaAs.

In the present work we have taken the coupled structure of the valence band into consideration, accounting for the degeneracy of the valence band and anisotropic exciton dispersion in bulk semiconductors. The scattering cross section in Eq. (25) is proportional to the product of density of final states and the square of the absolute value of the exciton-phonon interaction matrix element. We accounted for the anisotropy of the exciton dispersion in the density of states, while the matrix elements were evaluated in the spherical approximation. The use of a linear coordinate transformation defined in Eqs. (8) and (14) allowed us to use the zero-orbital-momentum component of the exciton wave function in the evaluation of the exciton-phonon interaction matrix elements in the FGR approximation for the exciton linewidth in Eq. (25).

We have included both deformation potential (DP) and piezoelectric (PE) interactions in our calculations, taking into account the tensor nature of the valence-band deformation potential. When the exciton self-energy is evaluated to the lowest order in exciton-phonon interaction (FGR approximation), the optical absorption has a Lorentzian shape with the linewidth given by Eq. (25). The resulting linewidths for bulk GaAs and ZnSe are close to the experimentally determined values.[5,29,30,31] The relative sizes of the DP and PE contributions to the linewidth depend on the value of the piezoelectric tensor component e_{14} and the effective exciton size a_{exc}. In the case of bulk GaAs the dominant contribution was found to come from PE interactions, while in the case of bulk ZnSe almost all contributions come from DP interactions.

Using the FGR results for exciton-phonon scattering rates in a degenerate band model, one can define an effective simple band isotropic mass and effective scalar deformation potential, Eq. (30). This effective mass depends on the interactions included in the model. Here we use actual DP and PE interactions, and the resulting value of $M^{\rm eff}$ is then used in the estimate of the effect of multiple-phonon scatterings on the exciton optical absorption. We have also included the effects of the exciton-impurity scattering in the evaluation of the exciton self-energy. The multiple-phonon scatterings were found to alter the absorption line shape, which can be noticeably non-Lorentzian at higher temperatures if the impurity induced linewidth $\Gamma(0)$ is small, smaller than 0.1 meV. However, the total multiple-phonon scattering contribution to the linewidth was found to be small compared to the one-phonon result—i.e., the one obtained from the FGR approximation, as shown in Fig. 1.

We have also considered exciton-phonon scattering effects on the optical linewidth in the case of the quantum wells sufficiently narrow to neglect the coupling of different subbands. In such cases a simple band model with isotropic in-plane exciton dispersion is applicable, and the resulting values of the HWHM were found to be compatible with the experimentally determined values for the GaAs/GaAlAs (Refs. 1 and 3–5) and ZnSe/ZnMgSSe (Refs. 31 and 41) systems. The contribution of the multiple-phonon scatterings in quasi-two-dimensional systems was found to be negligible. Comparing the acoustic-phonon-induced linewidths for narrow quantum wells with the bulk values calculated in the present work, we obtain a qualitative understanding of the experimentally observed size dependence of the exciton linewidths.[29]

ACKNOWLEDGMENTS

S.R. acknowledges useful discussions with B. Gelmont and T.L.R. those with M. Cardona and T. Ruf. This work was

supported in part by DARPA (S.R. and T.L.R.) and ONR (T.L.R.).

APPENDIX A: EXCITONS IN THE SPHERICAL APPROXIMATION

Evaluation of various matrix elements and approximations for the exciton eigenstates are conveniently done if the Hamiltonian is rewritten in terms of the irreducible spherical tensor operators.[15,17] First, after the coordinate transformation in Eq. (8) the exciton Hamiltonian in Eq. (7) takes the form

$$H_{\rm SP}=\left(\frac{1}{m_c}+\frac{1}{\tilde{m}}\right)\frac{p^2}{2}-\frac{e^2}{4\pi\varepsilon\varepsilon_f r}-\frac{\gamma}{m_0}(\mathbf{p}\cdot\mathbf{J})^2 +\left(\frac{\alpha_e^2}{2m_c}+\frac{\alpha_h^2}{2\tilde{m}}\right)\mathbf{P}_T^2+\left(\frac{\alpha_e}{m_c}-\frac{\alpha_h}{\tilde{m}}\right)\mathbf{p}\cdot\mathbf{P}_T -\frac{\gamma}{m_0}\alpha_h^2(\mathbf{P}_T\cdot\mathbf{J})^2+2\alpha_h\frac{\gamma}{m_0}(\mathbf{p}\cdot\mathbf{J})(\mathbf{P}_T\cdot\mathbf{J}), \quad \text{(A1)}$$

where $1/\tilde{m}=(\gamma_1+5\gamma/2)/m_0$, $\mathbf{P}_T$ is the total momentum with eigenvalues $\hbar\mathbf{K}$, and $\mathbf{p}$ is the relative momentum of the electron-hole pair.

Define the Cartesian second-rank tensor operators[17,26]

$$P_{ij}=3p_ip_j-\delta_{ij}p^2,$$

$$J_{ij}=\frac{3}{2}(J_iJ_j+J_jJ_i)-\delta_{ij}J^2, \quad \text{(A2)}$$

and the corresponding spherical tensor components for the first-rank and second-rank irreducible spherical tensors:

$$P_0^{(1)}=\frac{1}{2}p_3, \quad P_{\pm1}^{(1)}=\mp\frac{\sqrt{2}}{4}(p_1\pm ip_2),$$

$$P_0^{(2)}=\sqrt{\frac{3}{2}}P_{33}, \quad P_{\pm1}^{(2)}=\mp(P_{13}\pm iP_{23}),$$

$$P_{\pm2}^{(2)}=\frac{1}{2}(P_{11}-P_{22}\pm 2iP_{12}). \quad \text{(A3)}$$

With the z axis chosen along $\mathbf{P}_T$, the exciton Hamiltonian in Eq. (A1) takes the form

$$H_{\rm SP}=\frac{p^2}{2\mu}-\frac{e^2}{\varepsilon r}-\frac{\gamma}{9m_0}(P^{(2)}\cdot J^{(2)})+\left(\frac{\alpha_e^2}{2m_c}+\frac{\gamma_1\alpha_h^2}{2m_0}\right)P_{T3}^2 +2\left(\frac{\alpha_e}{m_c}-\frac{\gamma_1\alpha_h}{m_0}\right)P_0^{(1)}P_{T3}-\frac{1}{3}\sqrt{\frac{2}{3}}\frac{\gamma\alpha_h^2}{m_0}J_0^{(2)}P_{T3}^2 -\frac{4}{3}\sqrt{\frac{5}{3}}\frac{\gamma\alpha_h}{m_0}[P^{(1)}\times J^{(2)}]_0^{(1)}P_{T3}, \quad \text{(A4)}$$

where

$$\frac{1}{\mu}=\frac{1}{m_c}+\frac{\gamma_1}{m_0}.$$

The total angular momentum is $\mathbf{J}_T=\mathbf{F}+\mathbf{s}=\mathbf{L}+\mathbf{J}+\mathbf{s}$, where $\mathbf{J}$ and $\mathbf{s}$ are spin-3/2 and -1/2 operators of the hole and electron, respectively, and L is the orbital angular momentum of the exciton. As in Eq. (10), we will use the notation M, μ, and ν for the projections of $\mathbf{F}$, $\mathbf{J}$, and $\mathbf{s}$. The angular momentum $\mathbf{J}_T$ does not commute with momentum $\mathbf{P}_T$, and the exciton Hamiltonian has nonzero matrix elements between exciton states with different values of F, even in a spherical approximation for the valence band. For the lowest-energy exciton state at a given value of P_T, rewrite Eq. (10) as

$$\Phi(\mathbf{r})=\sum_i R_i(r)|L_i,J,F_i,M\rangle, \quad \text{(A5)}$$

with $|L_i-J|\leqslant F_i\leqslant L_i+J$. The Hamiltonian in Eq. (A4) has an axial symmetry, and M is constant in the eigenstate expansion. We restrict the basis states to those that couple to the $L=0$ state directly—i.e., in first order of H.[15] In the $M=\pm3/2$ subspaces, the basis consists of four states, corresponding to $L=0,1,1,2$ and $F=3/2,3/2,5/2,3/2$. In the $M=\pm1/2$ subspaces, the basis consists of five states, corresponding to $L=0,1,1,1,2$ and $F=3/2,1/2,3/2,5/2,3/2$. Matrix elements of various terms in Eq. (A4) can be evaluated using the Wigner-Eckart theorem and relations or tables for $3j$ and $6j$ symbols.[11,22,23]

The ground state, which will be referred to as the $1s$ state, will have the largest contribution from the $|0,3/2,3/2,M\rangle$ state. In any particular subspace with a given value of M, we can eliminate the coupling of this state to the $|1,3/2,3/2,M\rangle$ state by a particular choice of the coefficients α_e and α_h, Eq. (14). Specifically, consider the $M=3/2$ subspace. The ground-state problem is reduced to a three-dimensional subspace spanned by the basis functions $|0,3/2,3/2,3/2\rangle$, $|2,3/2,3/2,3/2\rangle$, and $|1,3/2,5/2,3/2\rangle$, resulting in three coupled linear differential equations for functions $R_i(r)$ in Eq. (A5), $i=0,1,2$. We will adopt a variational approach, with

$$R_0(r)=A\alpha^{3/2}e^{-\alpha r}, \quad R_2(r)=B\beta^{5/2}re^{-\beta r},$$

$$R_1(r)=iC\xi^{5/2}re^{-\xi r}. \quad \text{(A6)}$$

These functions have the correct behavior at small r, which follows from the differential equations. The normalization gives $A^2+3B^2+3C^2=4$. One can then show that with the parameters appropriate for GaAs and ZnSe, Table I, the function R_2 is an order of magnitude smaller than R_0, and the function R_1 is even smaller, unless K/α is very large. Therefore we are justified in using the $L=0$ wave function in the evaluation of the exciton-phonon matrix elements in Eqs. (16) and (23).

APPENDIX B: EVALUATION OF EXCITON-PHONON VERTEX TERMS IN THE PERTURBATION THEORY OF THE EXCITON SELF-ENERGY

As we already pointed out in Sec. IV, we use an effective simple exciton band model to estimate the contributions of the multiple-phonon scatterings to the optical absorption. The contribution of the self-consistent terms to the exciton self-energy is shown in the first line of Fig. 4. The thin

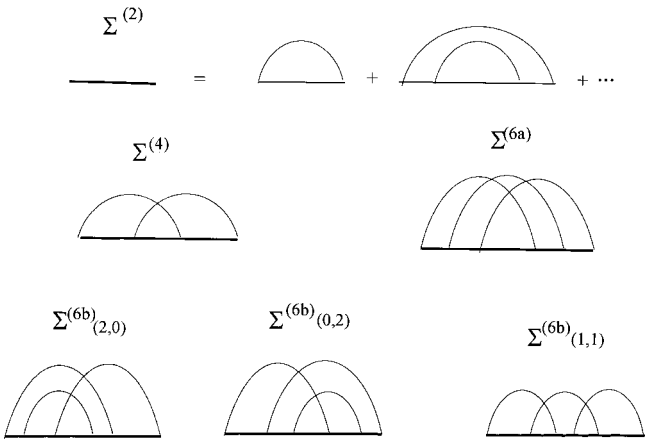

FIG. 4. Graphic representation of the terms in the perturbation series for the exciton self-energy. The thin straight lines represent the bare exciton propagator, and the thin curved lines represent the phonon propagators with the thermal average taken over the phonon occupation. The thick straight lines represent the exciton propagator renormalized by the self-consistent terms. The second and third lines show the first few vertex corrections of the type taken into account in Eq. (B15).

straight lines represent the bare exciton propagator, and the thin curved lines represent the phonon propagators with the thermal average taken over the phonon occupation.[12] Therefore, every phonon line carries a factor of $N_\tau(\mathbf{q})$ for phonon absorption and a factor $N_\tau(\mathbf{q})+1$ for phonon emission. Correspondingly, each diagram with n phonon lines represents 2^n terms. The thick straight lines represent the exciton propagator renormalized by the self-consistent terms. Each unrenormalized diagram of the fourth and higher order in the first line of Fig. 4 diverges, but their sum is finite.

It is convenient to use dimensionless variables here. We define a dimensionless momentum $\mathbf{x}$ so that

$$\hbar^2\mathbf{q}^2/2M_{\rm eff}=\mathbf{x}^2W, \tag{B1}$$

where W is some energy scale and we set $W=1$ meV. We define a dimensionless form factor for the effective deformation potential interaction as

$$F_{\rm DP}(x)=\frac{1}{(1+\lambda\alpha_h^2x^2)^2}-\frac{D_v^{\rm eff}/D_c}{(1+\lambda\alpha_e^2x^2)^2}, \tag{B2}$$

where $\lambda\equiv a_{\rm exc}^2M_{\rm eff}W/2\hbar^2$ and the dimensionless form factor for the piezoelectric interaction is given by

$$F_{\rm PE}(x)=\frac{1}{(1+\lambda\alpha_h^2x^2)^2}-\frac{1}{(1+\lambda\alpha_e^2x^2)^2}. \tag{B3}$$

The dimensionless energy relative to the unrenormalized exciton band edge and the dimensionless self-energy are defined as $\delta e\equiv(\hbar\omega-E_{1s})/W$ and $\sigma\equiv\Sigma/W$. We also define the exciton propagators for each phonon polarization:

$$G_\tau(\delta e,\sigma,x)=\sum_{\varsigma=\pm1}\frac{1}{\delta e-\sigma-x^2+\varsigma c_\tau x+i\gamma}, \tag{B4}$$

where $c_\tau\equiv(2v_\tau^2M_{\rm eff}/W)^{1/2}$ and $\gamma\equiv\Gamma(0)/W$ is included in order to account for impurity scattering. Neglecting the spontaneous-phonon emission, we obtain from Eq. (31), after integrating over the angles,

$$\sigma^{(2)}=\frac{k_BT}{W}\left\{\frac{D_c^2(2M)^{3/2}}{2\pi^2W^{1/2}\hbar^3\rho v_{\rm LA}^2}\int_0^\infty dx\,x^2F_{\rm DP}^2(x)G_L(\delta e,\sigma,x)+\frac{6(2M)^{1/2}}{35\pi^2W^{1/2}\hbar\rho v_{\rm LA}^2}\left(\frac{ee_{14}}{\varepsilon\varepsilon_f}\right)^2\int_0^\infty dx\,F_{\rm PE}^2(x)\times\left[G_L(\delta e,\sigma,x)+\frac{4}{3}\frac{v_{\rm LA}^2}{v_{\rm TA}^2}G_T(\delta e,\sigma,x)\right]\right\}. \tag{B5}$$

From this equation, we find the self-consistent approximation for the self-energy by replacing σ by $\sigma^{(2)}$ in the exciton propagators on the right-hand side. The corresponding self-energy $\Sigma^{(2)}(\omega)$ is used then in Eq. (29) to obtain the absorption line shape $\alpha(\omega)$ at this level of approximation.

In order to simplify the evaluation of the vertex terms, we approximate the sound velocity in the exciton propagators for different polarizations by one value $v_{\rm LA}$ and c_τ by $c\equiv c_{\rm LA}$. This allows us to combine the DP and PE terms in the following way. By using the angularly averaged PE interaction, the following modified PE form factor can be defined,

$$\tilde F_{\rm PE}(x)=\sqrt{\frac{12}{35}}\frac{ee_{14}}{\varepsilon\varepsilon_fD_c}\left(\frac{\hbar^2}{2M_{\rm eff}W}\right)^{1/2}\left(1+\frac{4}{3}\frac{v_{\rm LA}^2}{v_{\rm TA}^2}\right)^{1/2}\frac{F_{\rm PE}(x)}{x}, \tag{B6}$$

and then we can define the total effective exciton form factor $\tilde F(x)$, so that

$$\tilde F^2(x)=F_{\rm DP}^2(x)+\tilde F_{\rm PE}^2(x). \tag{B7}$$

The first diagram in the second line in Fig. 4 represents the four lowest-order vertex terms in the perturbation series for the self-energy. The evaluation is similar to that for the elastic scattering.[34] The momentum integrals can be evaluated in spherical coordinates. The angular integrations are elementary, and one is left with a double integral over the absolute values of two phonon momenta. The sum over the four terms in $\Sigma^{(4)}$ can be rewritten so that the integrand is an even function of the phonon momenta x_1 and x_2. This allows us to extend the x_2 integration to the $(-\infty,\infty)$ interval. We obtain then

$$\sigma^{(4)}=2\left(\frac{k_BT}{W}\right)^2J^2\int_0^\infty dx_1x_1\tilde F^2(x_1)\times\left[\frac{I(x_1)}{\delta e-\sigma-x_1^2-cx_1+i\gamma}-\frac{I(-x_1)}{\delta e-\sigma-x_1^2+cx_1+i\gamma}\right], \tag{B8}$$

where

$$J \equiv \frac{D_c^2 (2M)^{3/2} W^{1/2}}{4\pi^2 \rho v_{\mathrm{LA}}^2 \hbar^3}, \tag{B9}$$

$$I(x_1) = \frac{1}{2} \int_{-\infty}^{\infty} dx_2 x_2 \tilde{F}^2(x_2) \frac{1}{\delta e - \sigma - x_2^2 - c x_2 + i\gamma} \times \ln\left[\frac{(x_1 - x_2)^2 + c(x_1 + x_2) - \delta e - \sigma}{(x_1 + x_2)^2 + c(x_1 + x_2) - \delta e - \sigma} \right]. \tag{B10}$$

The integral $I(x_1)$ can be evaluated in the complex plane. The integrand has poles from the propagator and cuts from the logarithm. The contributions from the poles of $F(x_2)$ have a small effect on the imaginary part of σ and will be ignored in this calculation. In this way we obtain

$$I(x_1) = -\frac{i\pi}{2} \tilde{F}^2(z_3) \left\{ \left(1 - \frac{c}{\sqrt{c^2 + 4(\delta e - \sigma + i\gamma)}} \right) \times \ln\left[\frac{(x_1 + c - 2z_3)(z_1 - z_3)}{(x_1 + c + 2z_3)(z_2 - z_3)} \right] - \left(1 + \frac{c}{\sqrt{c^2 + 4(\delta e - \sigma + i\gamma)}} \right) \ln\left(\frac{z_1 - z_4}{z_2 - z_4} \right) \right\}, \tag{B11}$$

where the branch of the logarithm is chosen which goes to zero in the double limit $c \to 0$, $x_1 \to 0$, and

$$z_{1,2} \equiv x_1 - \frac{c}{2} \pm \sqrt{\frac{c^2}{4} + \delta e - \sigma + i\gamma - 2c x_1},$$

$$z_{3,4} \equiv -\frac{c}{2} \pm \sqrt{\frac{c^2}{4} + \delta e - \sigma + i\gamma}. \tag{B12}$$

To fourth order in exciton-phonon interaction, the dimensionless self-energy as a function of the dimensionless energy shift δe is found as the solution of the transcendental equation $\sigma = \sigma^{(2)}(\sigma) + \sigma^{(4)}(\sigma)$. From numerical evaluation we find that no significant error will be made in the absorption if we approximate $I(x)$ by its elastic limit[34] $I_{\mathrm{el}}(x)$ in Eq. (B8), while keeping $c \neq 0$ in the remaining propagators. In doing this, we also replace $\tilde{F}^2(z_3)$ by half of its maximum value—i.e., by $(1/2)\tilde{F}^2(0)$. Then we obtain a simpler expression

$$I_{\mathrm{el}}(x_1) = -\frac{i\pi}{2} \tilde{F}^2(0) \ln\left[\frac{(\delta e - \sigma + i\gamma)^{1/2} - x_1/2}{(\delta e - \sigma + i\gamma)^{1/2} + x_1/2} \right], \tag{B13}$$

to be used in Eq. (B8).

Turning to the higher-order terms, the terms in the perturbation expansion proliferate rapidly, and we will confine ourselves to the two classes of diagrams considered by Toyozawa.[34] In the sixth order, the "maximally crossed" diagram is the second one in the second line of Fig. 4. It represents eight terms as every phonon line can describe either the emission or absorption of one phonon. The three diagrams in the third line of the same figure represent 24 terms of the other class. In the approximation of Eq. (B13) the diagrams of the order $2n$ add up to give

$$\sigma^{(2n)}(n \geqslant 3) = 2\left(\frac{k_B T}{W} \right)^n (n+1) J^n \int_0^{\infty} dx\, x \tilde{F}^2(x) \times \left[\frac{x^{2-n} I^{n-1}(x)}{\delta e - \sigma - x^2 - cx + i\gamma} - \frac{(-x)^{2-n} I^{n-1}(-x)}{\delta e - \sigma - x^2 + cx + i\gamma} \right], \tag{B14}$$

with J defined in Eq. (B9). The transcendental equation for self-energy σ as a function of the energy shift δe is obtained as

$$\sigma = \sum_{n=1}^{\infty} \sigma^{(2n)}(\sigma). \tag{B15}$$

The equation for the self-energy Σ does not of course depend on the choice of the energy scale W. Numerical solution of Eq. (B15) is used in the expression for absorption α to obtain the line shapes shown in Fig. 2.

APPENDIX C: EFFECT OF THE PHONON-INDUCED MOTION OF IMPURITIES ON THE TEMPERATURE-DEPENDENT LINEWIDTH

Lattice vibrations cause imbedded impurities to move, and the scattering of electrons and holes by the moving impurities is not elastic in the stationary coordinate system.[37] The resulting exciton–acoustic-phonon interaction Hamiltonian will have "three-body" electron-phonon-impurity terms. In the lowest-order approximation for the exciton self-energy—i.e., the FGR—the contribution of these terms to the exciton linewidth is proportional to the number of acoustic phonons, thus contributing to the linear temperature dependence in Eq. (1). In the case of impure metals, an electron-phonon model Hamiltonian was derived in Ref. 38. We consider here a similar model for the carrier-phonon interaction in the case of a direct band-gap semiconductor in a simple band effective mass approximation for the motion of carriers in the periodic field of the lattice and considering longitudinal acoustic phonons.

Let us assume there are N_{imp} impurities at the lattice sites $\mathbf{R}_i$ and that the interaction of electrons in both conduction and valence bands with impurities is given by the potentials $u_{\mathrm{imp}}(\mathbf{r}_\alpha - \mathbf{R}_i)$, $\alpha = e, h$. The effective masses of the electrons and holes are m_e and m_h, respectively. The wave functions of the relative electron-hole motion are $\phi_\lambda(\mathbf{r})$, where index λ labels different exciton states. In the low-carrier-density limit, the three-body interaction is obtained as

$$H' = H_{\text{ex-ph-imp}} = \frac{1}{\sqrt{2V}} \sum_{\lambda, \lambda', \mathbf{p}, \mathbf{q}, \mathbf{k}} U_{\lambda\lambda'}(\mathbf{q}) u_{\mathrm{imp}}(\mathbf{q}) f(\mathbf{q}, \mathbf{k}) \times \hat{B}^+_{\lambda'}(\mathbf{p} + \mathbf{q}) \hat{B}_\lambda(\mathbf{p}) (\hat{a}_{\mathbf{k}} + \hat{a}^+_{-\mathbf{k}}), \tag{C1}$$

where $\hat{B}$ and $\hat{a}$ are exciton and phonon annihilation operators, $u_{\rm imp}(\mathbf{q})$ is the Fourier transformation of $u_{\rm imp}(\mathbf{r})$, $f(\mathbf{q},\mathbf{k})$ depends on equilibrium positions of the impurities and is defined as

$$f(\mathbf{q},\mathbf{k})=\frac{q}{\sqrt{V\rho\omega(k)}}\sum_i e^{-i(\mathbf{q}-\mathbf{k})\cdot R_i^0}. \tag{C2}$$

$U_{\lambda'\lambda}(\mathbf{q})$ is the exciton form factor given by

$$U_{\lambda\lambda'}(\mathbf{q})=\int d^3r(e^{i\mathbf{q}\cdot\mathbf{r}m_h/M}-e^{-i\mathbf{q}\cdot\mathbf{r}m_e/M})\phi^*_{\lambda'}(\mathbf{r})\phi_\lambda(\mathbf{r}). \tag{C3}$$

$M=m_e+m_h$, and V is the volume. The configuration-dependent exciton-phonon matrix element is given by

$$V_{\lambda\lambda'}(\mathbf{q},\mathbf{k};\{\mathbf{R}_i^0\})=U_{\lambda\lambda'}(\mathbf{q})u_{\rm imp}(\mathbf{q})f(\mathbf{q},\mathbf{k}). \tag{C4}$$

Consider the intraband transitions $\lambda'=\lambda=1s$. The corresponding exciton wave function is $\phi_{1s}(r)=(\pi a_{\rm exc}^3)^{-1/2}\exp(-r/a_{\rm exc})$, where $a_{\rm exc}$ is the exciton Bohr radius. From Eq. (C3) we obtain

$$U_{1s}(q)=\frac{1}{(1+q^2a_{\rm exc}^2m_h^2/4M^2)^2}-\frac{1}{(1+q^2a_{\rm exc}^2m_e^2/4M^2)^2}. \tag{C5}$$

In the FGR approximation, the exciton linewidth Γ_{1s} is obtained as the imaginary part of the exciton self-energy at the band edge. After taking a thermal average over the phonon distribution and a configurational average over the positions of impurities, we obtain

$$\Gamma'_{1s}=\frac{\pi}{2}\hbar\sum_{kqq'}\langle V_{1s}(\mathbf{q},\mathbf{k};\{\mathbf{R}_i^0\})V_{1s}(\mathbf{q}',\mathbf{k};\{\mathbf{R}_i^0\})\rangle \times N_{\rm ph}(k)\delta\left(\frac{\hbar^2k^2}{2M}-\hbar kv_{\rm LA}\right), \tag{C6}$$

where $N_{\rm ph}(k)$ is the Bose function for phonons. To the linear order in impurity density $n_{\rm imp}=N_{\rm imp}/V$, we obtain

$$\Gamma'_{1s}=\frac{k_BTn_{\rm imp}}{8\pi\hbar\rho v_{\rm LA}^3}\int\frac{d^3q}{(2\pi)^3}|U_{1s}(q)|^2|u_{\rm imp}(q)|^2q^2. \tag{C7}$$

Various possible approximations for the matrix element $u_{\rm imp}(q)$ result in Γ' a few orders of magnitude smaller than the linewidth obtained from the exciton-phonon interaction evaluated in the same approximation. Here we will discuss two different models. In the first one, we consider a statically screened Coulomb potential $u_{\rm imp}(q)=e^2/4\pi\varepsilon_f\varepsilon q^2$. For $n_{\rm imp}\sim10^{18}$ cm^{-3} we find from Eq. (C7) that $\Gamma'/k_BT\sim10^{-7}-10^{-6}$. In the second model, we consider a short-range scattering of strength u_0. Then the result of Eq. (C7) can be expressed in terms of Γ_0, which we define here as the sum of impurity-induced electron and hole linewidths evaluated at the energy corresponding to the electron-hole relative motion in the exciton bound state. One can easily show that $\Gamma_0=n_{\rm imp}u_0^2M/2\pi a_{\rm ex}\hbar^2$. In terms of Γ_0, we obtain from Eq. (C7) that $\Gamma'/k_BT\sim(\Gamma_0/1\ \text{meV})\times10^{-5}$. As Γ_0 is usually smaller than 1 meV, the result is a negligible contribution to the temperature dependence of the linewidth.

[1] D. Gammon, S. Rudin, T. L. Reinecke, D. S. Katzer, and C. S. Kyono, Phys. Rev. B **51**, 16 785 (1995).

[2] C. Weisbuch and R. G. Ulbrich, in *Light Scattering in Solids III*, edited by M. Cardona and G. Guntherodt (Springer-Verlag, Berlin, 1982), pp. 207–263.

[3] T. Ruf, J. Spitzer, V. F. Sapega, V. I. Belitsky, M. Cardona, and K. Ploog, Phys. Rev. B **50**, 1792 (1994).

[4] P. Borri, W. Langbein, J. M. Hvam, and F. Martelli, Phys. Rev. B **59**, 2215 (1999).

[5] A. V. Gopal, R. Kumar, A. S. Vengurlakar, A. Bosacchi, S. Franchi, and L. N. Pfeiffer, J. Appl. Phys. **87**, 1858 (2000).

[6] Piermarocchi, F. Tassone, V. Savona, A. Quattropani, and P. Schwendimann, Phys. Rev. B **53**, 15 834 (1996).

[7] Y. Toyozawa, Prog. Theor. Phys. **20**, 53 (1958).

[8] S. Rudin, T. L. Reinecke, and B. Segall, Phys. Rev. B **42**, 11 218 (1990).

[9] S. Rudin and T. L. Reinecke, Phys. Rev. A **62**, 053806 (2000).

[10] V. Pellegrini, R. Colombelli, L. Sorba, and F. Beltram, Phys. Rev. B **59**, 10 059 (1999).

[11] L. D. Landau and E. M. Lifshitz, *Quantum Mechanics—Nonrelativistic Theory* (Pergamon, London, 1965).

[12] B. M. Agranovich, *Theory of Excitons* (in Russian) (Nauka, Moscow, 1968).

[13] V. F. Gantmakher and Y. B. Levinson, *Carrier Scattering in Metals and Semiconductors* (North-Holland, Amsterdam, 1987).

[14] E. O. Kane, Phys. Rev. B **11**, 3850 (1975).

[15] M. Altarelli and N. O. Lipari, Phys. Rev. B **15**, 4898 (1977).

[16] S. Rudin and T. L. Reinecke, Phys. Rev. B **65**, 121311 (2002).

[17] N. O. Lipari and M. Altarelli, Phys. Rev. B **15**, 4883 (1977).

[18] U. Roessler, in *Festkoerperprobleme Advances in Solid State Physics XIX*, edited by J. Treusch (Vieweg, Braunscweig, 1979), p. 77.

[19] J. M. Luttinger and W. Kohn, Phys. Rev. **97**, 869 (1955).

[20] A. P. Silin, Sov. Phys. Solid State **13**, 1494 (1971).

[21] B. L. Gelmont, S. B. Sultanov, and Al. L. Efros, Sov. Phys. Semicond. **18**, 1380 (1984).

[22] A. R. Edmonds, *Angular Momentum in Quantum Mechanics* (Princeton University Press, Princeton, 1960).

[23] D. A. Varshalovich, A. N. Moskalev, and V. K. Khersonskii, *Quantum Theory of Angular Momentum* (World Scientific, Singapore, 1988).

[24] N. O. Lipari and A. Baldareschi, Phys. Rev. Lett. **25**, 1660 (1970).

[25] B. L. Gelmont and M. I. Dyakonov, Sov. Phys. Semicond. **5**, 1905 (1972).

[26] A. Baldereschi and N. O. Lipari, Phys. Rev. B **8**, 2697 (1973).

[27] G. L. Bir and G. E. Pikus, Sov. Phys. Solid State **2**, 2039 (1960).

[28] G. L. Bir, E. Normantas, and G. E. Pikus, Sov. Phys. Solid State **4**, 867 (1962).
[29] L. Schultheis, A. Honold, J. Kuhl, K. Köhler, and C. W. Tu, Phys. Rev. B **34**, 9027 (1986).
[30] A. Tredicucci, Y. Chen, F. Bassani, J. Massies, G. Deparis, and G. Neu, Phys. Rev. B **47**, 10 348 (1993).
[31] C. W. Chang, H. C. Yang, C. H. Chen, H. J. Chang, and Y. F. Chen, J. Appl. Phys. **89**, 3725 (2001).
[32] S. Adachi, J. Appl. Phys. **58**, R1 (1985).
[33] D. D. Nolte, W. Walukiewicz, and E. E. Haller, Phys. Rev. Lett. **59**, 501 (1987).
[34] Y. Toyozawa, Prog. Theor. Phys. **27**, 89 (1962).
[35] D. Pines, in *Polarons and Excitons*, edited by C. G. Kuper and G. D. Whitfield (Plenum, New York, 1963), p. 155.
[36] W. C. Tait and R. L. Weither, Phys. Rev. **166**, 769 (1968).
[37] T. Tsuneto, Phys. Rev. **121**, 402 (1961).
[38] G. Grünewald and K. Scharnberg, Z. Phys. **268**, 197 (1974).
[39] S. Rudin and T. L. Reinecke, Phys. Rev. B **41**, 3017 (1990).
[40] S. L. Chuang, *Physics of Optoelectronic Devices* (Wiley, New York, 1995).
[41] J. Suda, Y. Kawakami, Sz. Fujita, and Sg. Fujita, Jpn. J. Appl. Phys., Part 2 **33**, L986 (1994).
[42] M. Ueta, H. Kanzaki, K. Kobayashi, Y. Toyozawa, and E. Hanamura, *Excitonic Processes in Solids* (Springer-Verlag, Berlin, 1986).
[43] *Semiconductors*, edited by O. Madelung, Landoldt-Börnstein New Series, Group III, Vols. 17a, 17b, and 22b (Springer, Berlin, 1982, 1986, 1987).
[44] A. J. Moses, *The Practicing Scientist Handbook* (Van Nostrand, New York, 1978).
[45] G. Arlt and P. Quadflieg, Phys. Status Solidi **25**, 323 (1968).
[46] D. Berlincourt, H. Jaffe, and L. R. Shinozawa, Phys. Rev. **129**, 1009 (1963).
[47] N. T. Pelecanos *et al.*, Phys. Rev. B **45**, 6037 (1992) S.-H. Wei and A. Zunger, *ibid.* **60**, 5404 (1999); A. Blacha *et al.*, Phys. Status Solidi B **126**, 11 (1984).